AD-A142 357 A COMPUTER MODEL FOR A MULTIPLE HIGH PRF PULSE DOPPLER RADAR(U) NAVAL RESEARCH LAB WSSHINGTON DC K GERLACH ET AL. 07 JUN 84 NRL-MR-5332 1/1

UNCLASSIFIED F/G 17/9 NL

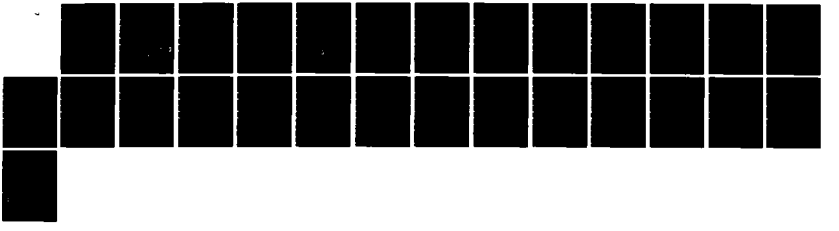

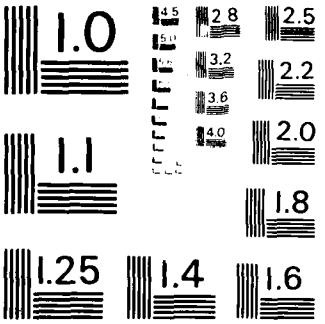

(2)

NRL Memorandum Report 5332

A Computer Model for a Multiple High PRF Pulse Doppler Radar

KARL GERLACH AND T. B. MITCHELL

Airborne Radar Branch
Radar Division

June 7, 1984

NAVAL RESEARCH LABORATORY
Washington, D.C.

REPORT DOCUMENTATION PAGE

1a REPORT SECURITY CLASSIFICATION UNCLASSIFIED	1b RESTRICTIVE MARKINGS
2a SECURITY CLASSIFICATION AUTHORITY	3 DISTRIBUTION AVAILABILITY OF REPORT Approved for public release; distribution unlimited
2b DECLASSIFICATION/DOWNGRADING SCHEDULE	
4 PERFORMING ORGANIZATION REPORT NUMBER(S) NRL Memorandum Report 5332	5 MONITORING ORGANIZATION REPORT NUMBER(S)
6a NAME OF PERFORMING ORGANIZATION Naval Research Laboratory 6b OFFICE SYMBOL (If applicable)	7a NAME OF MONITORING ORGANIZATION Naval Electronic Systems Command
6c ADDRESS (City, State, and ZIP Code) Washington, DC 20375	7b ADDRESS (City, State, and ZIP Code) Washington, DC 20360
8a NAME OF FUNDING/SPONSORING ORGANIZATION Naval Electronic Systems Command 8b OFFICE SYMBOL (If applicable)	9 PROCUREMENT INSTRUMENT IDENTIFICATION NUMBER
8c ADDRESS (City, State, and ZIP Code) Washington, DC 20360	10 SOURCE OF FUNDING NOS PROGRAM ELEMENT NO: 62712N; PROJECT NO:; TASK NO: XF12-141-100; WORK UNIT NO: DN380-101
11 TITLE (Include Security Classification) (See Page ii)	
12 PERSONAL AUTHOR(S) Gerlach, Karl and Mitchell, T.B.	
13a TYPE OF REPORT Interim 13b TIME COVERED FROM TO	14 DATE OF REPORT (Yr, Mo, Day) 1984 June 7 15 PAGE COUNT
16 SUPPLEMENTARY NOTATION	

17 COSATI CODES			18 SUBJECT TERMS (Continue on reverse if necessary and identify by block number)		
FIELD	GROUP	SUB GR	Pulse Doppler	Post Detecting Processing	Simulation
			Multiple PRF	Square Law Detector	Radar
			Detectors	Binary Detector	

19 ABSTRACT (Continue on reverse if necessary and identify by block number)

A computer model which simulates a Multiple High PRF Pulse Doppler radar has been developed. The model has the capability of computing the system parameters for Post Detection Processing necessary to achieve given desired probabilities of detection and false alarm. A variety of parameters such as range resolution, number of PRF bursts, number of doppler bins, and Swerling model are inputted. Output measures of effectiveness include the required signal-to-noise power ratio per pulse burst, average number of a arithmetic operations, and ghosting probabilities.

20 DISTRIBUTION/AVAILABILITY OF ABSTRACT UNCLASSIFIED/UNLIMITED X SAME AS RPT ☐ DTIC USERS ☐	21 ABSTRACT SECURITY CLASSIFICATION UNCLASSIFIED
22a NAME OF RESPONSIBLE INDIVIDUAL Karl Gerlach	22b TELEPHONE NUMBER (Include Area Code) 202-767-3475 22c OFFICE SYMBOL 5367

DD FORM 1473, 83 APR EDITION OF 1 JAN 73 IS OBSOLETE

11. TITLE (Include Security Classification)

A Computer Model for a Multiple High PRF
Pulse Doppler Radar

CONTENTS

A COMPUTER MODEL FOR A MULTIPLE HIGH PRF PULSE DOPPLER RADAR

I. INTRODUCTION

A characteristic of a high PRF radar is that its maximum unambiguous detection range, R_{MAX}, is much smaller than the desired detection range. Thus, it is not possible to measure the true range to a target beyond R_{MAX} using an unmodulated pulse burst at one PRF. However by using one or more PRF's, it possible to determine the true range to a target by using some multiple PRF ranging technique [1-3].

A detection methodology associated with multiple high PRF radars has been reported in Ref. [4]. The purpose of this report is to describe in detail the computer modeling associated with this detection methodology. This processing technique can be applied to the analysis of either Airborne or Space-based radars. We refer to the processor of the radar returns of the multiple high PRF pulse doppler radar as the Post Detection Processor.

II. POST DETECTION PROCESSOR

The basic Post Detection Processor (PDP) is illustrated in Fig. 1. The processor actually consists of multiple processors. The first PDP resolves the range ambiguities. Unfortunately, in order to resolve the range ambiguities, a suboptimal detector (a binary detector) for a given false alarm rate is employed. The second PDP is the near optimal detector for a given false alarm rate. This detector consists of incoherently integrating (or summing) the squared magnitude of the voltage returns for each PRF and associated range-doppler bins where the target return is present (the output of the coherent integrators). Next, this sum is compared against a threshold (determined by the desired false alarm rate). If the sum is greater than this threshold a candidate target is declared. Because ghosts can be generated by the association process involved with finding a target's unambiguous range, a Deghosting Algorithm is employed to eliminate a large percentage of these ghosts while at the same time eliminating only a small percentage of real targets. Deghosting is discussed further in Appendix D and Ref. [3].

Besides resolving the range ambiguities, the first PDP also screens potential candidate data for the second PDP. A target must be detected in the first PDP in order to be considered for detection in the second PDP. Hence, the first PDP aids in reducing the amount of data that must be processed by the second PDP. Due to the large number of range-doppler bins, the gating of the data into the second PDP is desirable.

An additional breakdown of the PDP is seen in Figs. 2, 3, and 4. In Fig. 2, V-MEM contains the raw voltage data from each range-doppler bin and each PRF. Each of these voltages are threshold detected and the results of this operation are contained in D-MEM (zeros indicating no detection, ones indicating detection for a single PRF, range-doppler bin). This data is inputted into the Range and Target Ambiguity Resolver (RTAR) as seen in Fig. 3. For each detection (in D-MEM) the PRF is

Manuscript approved March 1, 1984.

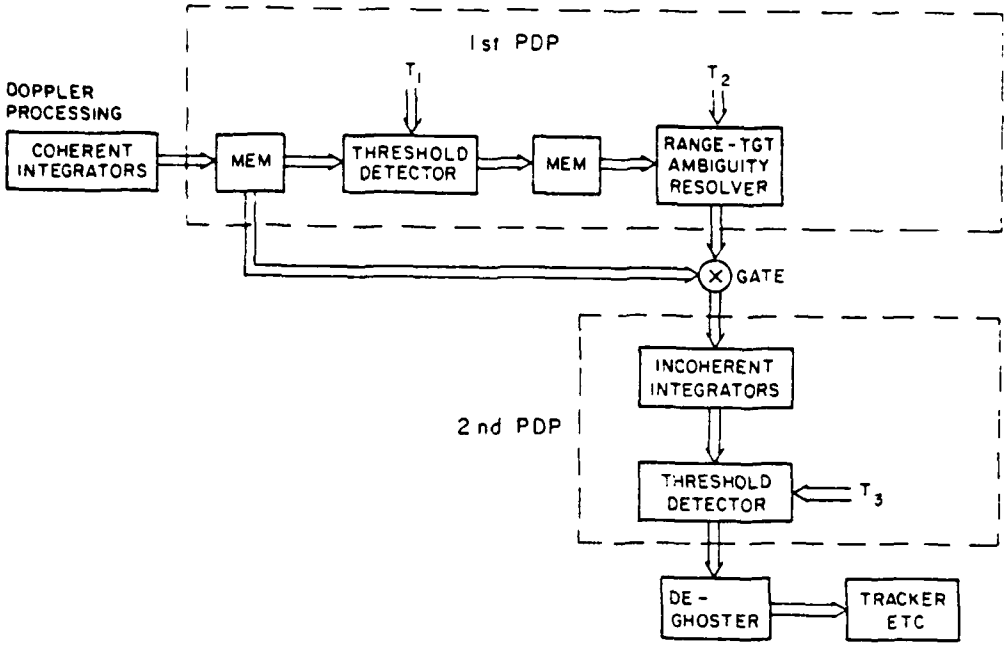

Fig. 1 — Basic PDP configuration

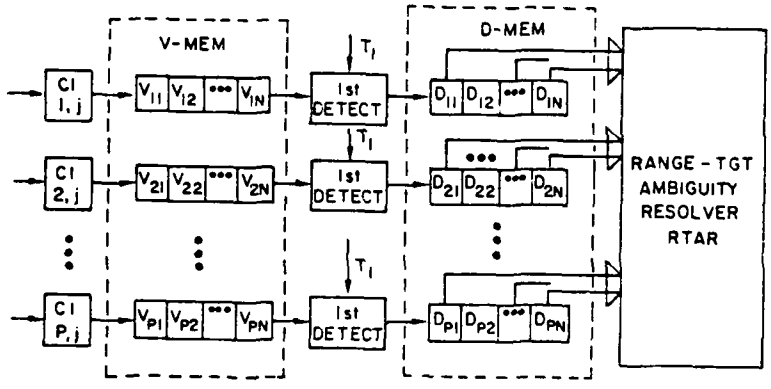

- CI i, j ≡ COHERENT INTEGRATOR OF THE i, j RANGE DOPPLER BIN. i = 1, 2, •••, P; j = 1, 2, •••, N_d
- P = NUMBER OF RANGE CELLS BETWEEN RANGE AMBIGUITIES
- N_d = NUMBER OF DOPPLER BINS
- N = NUMBER OF BURSTS AT DIFFERENT PRF'S

Fig. 2 — First stage of the PDP

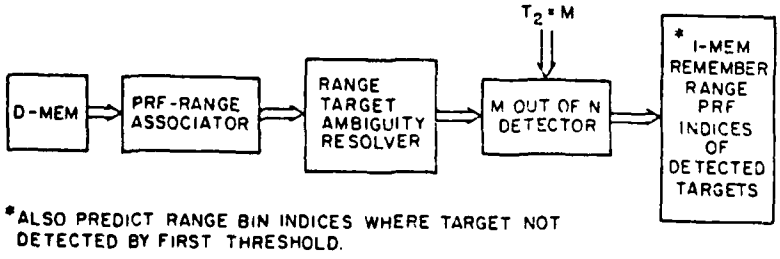

*ALSO PREDICT RANGE BIN INDICES WHERE TARGET NOT DETECTED BY FIRST THRESHOLD.

Fig. 3 — Range target ambiguity resolver

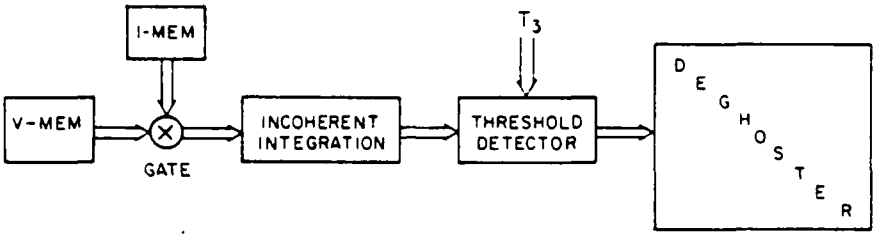

Fig. 4 — Second PDP and deghoster

correlated (or associated) with an ambiguous range. These are sorted out by a Range and Ambiguity Resolver algorithm which attempts to:

- find the unambiguous range of the real targets
- distinguish between two or more targets that fall within a given doppler velocity

A requirement of the detection methodology reported in [4] is that only two PRF bursts are necessary in order to calculate the true range of a detected target. By this we mean that the range extent of the radar's mainbeam footprint is such that any two of the PRF bursts can determine the unambiguous range of a given target assuming that the returns from the two PRF's are above the first level threshold. If more than two PRF burst are used, then the extra PRF's are used to resolve target ambiguities that can occur when more than one target is in a given doppler bin. Note that if this redundancy did not exist the target ambiguities could not be resolved and false alarms (ghosts) would be generated. A more complete description of the PRF ranging techniques and the Range Target Ambiguity Algorithm can be found in Appendices A and B.

A *M out of N binary* detector determines whether a set of returns is passed to the second PDP as seen in Fig. 4. Hence, we see that a binary detector is embedded in the first PDP and that this detector is cascaded with a square law detector. The thresholds, T_1, T_2 and T_3, seen in Figs. 2-4 can be determined apriori if the desired probabilities of false alarm and detection at the output of the square law detector and the target model (Swerling case) are specified. Further discussion on these thresholds are found in Appendix C and Ref. [4]. If the internal noise level is not known apriori (which is normally the case) then some sort of Constant False Alarm Rate (CFAR) procedure can be implemented by which the internal noise level is estimated and the thresholds are set accordingly.

III. TRADEOFFS

One of the fundamental tradeoffs in the design of Multiple High PRF Pulse Doppler Radar is number of operations per second (NOP's/SEC) that the processor must perform versus the minimum required signal-to-noise power ratio per pulse burst needed for a specified detection probability, false alarm probability, and target type (Swerling model). It will be found that one increases as the other decreases (or one measure of effectiveness worsens as the other improves). To illustrate this point it can be shown that the first PDP (with the embedded binary detector) seen in Fig. 1 is not necessary in order to extract the unambiguous range of a target. A functional block diagram of an algorithm that employs only the second PDP (the square law detector) and resolves the range ambiguities is illustrated in Fig. 5.

For each doppler bin, the outputs of the coherent integrators are stored in a memory, VMEM, where the components of this memory are indexed vertically by the contiguous ambiguous ranges and horizontally by the PRF bursts. The Sequential Range Selector seen in this figure works as follows: for each unambiguous range in the radar's mainbeam footprint, $R = R_0 + K\Delta R$, $K = 0, 1, 2, \ldots,$ KMAX, the ambiguous ranges associated with R are calculated with respect to the various PRF's used.

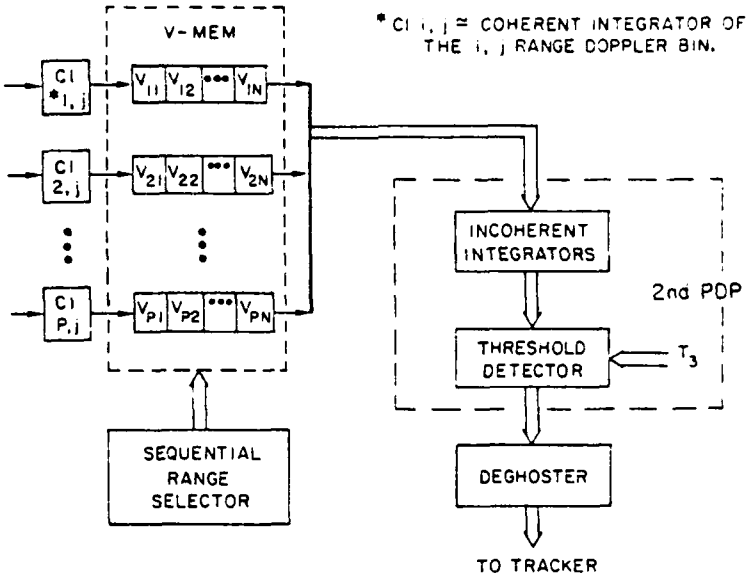

Fig. 5 — PDP without binary detector

The ambiguous ranges and their respective PRF's are then used as indices to form memory addresses to V-MEM. These addresses are used to fetch the stored returns from V-MEM to the incoherent integrator and threshold detector of the second PDP. Hence, for a selected unambiguous range, if the threshold of the detector is passed then a detection is declared in that unambiguous range bin. The unambiguous ranges are stepped sequentially until all have been tested for detections.

The penalty for using this scheme is that the number of software operations (NOP's) that must be performed each dwell time will be large. The NOP's will be proportional to the product of the number of doppler bins, N_d, the number of unambiguous range bins, N_r, in the footprint, and the number of pulse bursts, N. For example, if $N_d = 100$, $N_r = 1200$ and $N = 4$, then NOP's $\sim$ 480,000.

If the first PDP is employed, the number of operations performed by the second PDP is greatly reduced. This results because the first PDP screens out many of the range-doppler cells from detectability consideration. However, the first PDP itself must perform a number of operations in order to pass data to the second PDP. Hence, the total number of operations used by both PDP's will be a function of the detectability characteristics of the first PDP.

If a minimum probability of detection, P_D, and maximum false alarm probability, P_{FA}, are set for data entering the first PDP and exiting the second PDP then the required $(S/N)_{req}$ and the total NOP's will be a function of P_D, P_{FA}, and the thresholds set in the first PDP (or equivalently the detectability characteristics of the first PDP). It can be shown that the maximum NOP's occur when the required $(S/N)_{req}$ is a minimum. This is the case where the first PDP passes everything. Hence, a tradeoff study of $(S/N)_{req}$ and the total NOP's versus the detection characteristics of the second PDP is identified.

The important parameter which influences the NOPs is the probability of false alarm through the binary detector, P_{FBD}. If this is set low, then very few false alarms (noise only) in D-MEM (see Fig. 2) occur so that the number of operations in the Range-Target Ambiguity Resolver Algorithm will be small resulting in a lower NOP's requirement. However, $(S/N)_{req}$ will be larger since the binary detector which is an inferior detector to the square law detector screens out most of the false alarms. If P_{FBD} is set high the NOP's will increase because of more false alarms in D-MEM.

Another fundamental tradeoff will be between the false alarm rate due to ghosting and the minimum required $(S/N)_{req}$. Again the parameter, P_{FBD}, plays an important role. As more candidate targets are passed through the binary detector (P_{FBD} increases), the ghosting rate will increase. As previously mentioned, the minimum required signal-to-noise ratio decreases as P_{FBD} increases.

The ghosting probability is also a function of many other parameters. This is discussed in more detail in Ref. [3].

IV. MODEL DESCRIPTION

The functional flow of the Post Detection Processor computer model (called PDPMOD) is shown in Fig. 6.

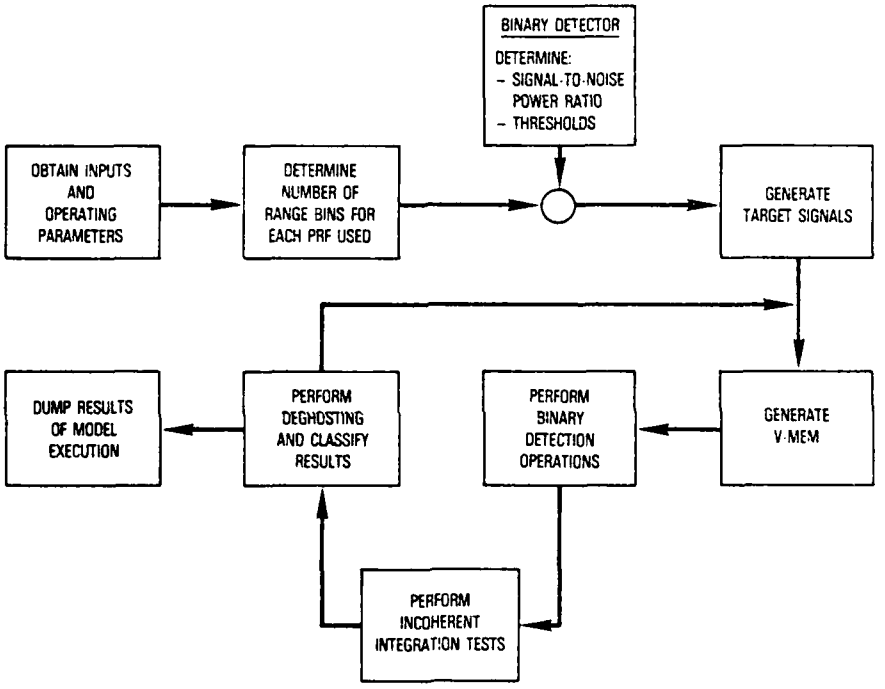

Fig. 6 — General flowchart

Initially, the user interacts in submitting the operating parameters which are used in defining the target environment and target model. The program will request an input for each of the following parameters:

- Desired quiescent probability of false alarm, P_F
- Desired probability of detection , P_D
- Quiescent probability of false alarm at the output of the binary detector, P_{FBD}
- Number targets in mainbeam footprint, N_t
- Number of doppler bins, N_d

- Range resolution
- Maximum operating range of the radar
- Number of PRF bursts
- Minimum value for M (M out of N binary detector)
- Swerling model of target
- Deghosting algorithm parameters
- Dwell time

As a function of these input parameters other system parameters are computed. These include

- The three thresholds, T_1, T_2, and T_3, of the cascaded detector (see Appendix C)
- The minimum required signal-to-noise power ratio $(S/N)_{req}$ needed to achieve the desired P_F and P_D (see Appendix C).
- Random number of targets inputted into a single doppler bin
- Each target's unambiguous range randomly selected
- The PRF's associated with the N PRF's.
- Number of unambiguous range bins, N_r, in the maximum operating range of the radar.

Next, target voltages associated with the calculated $(S/N)_{req}$ and target Swerling model are generated for each target. If there are N PRF pulse bursts, then each target will have N voltage returns associated with itself. These voltages are added to a zero mean gaussian noise voltage whose power is normalized to one. These sums are placed into the respective ambiguous range bins in V-MEM as seen in Fig. 2 for each PRF burst. Ambiguous range-PRF cells as seen in Fig. 2 which contain no target returns are filled with "noise only" voltages.

After V-MEM is filled, the Post Detection processing continues as described in Section II.

Bookkeeping routines count the occurance of the detection, false alarm, and ghosting events. In addition, the number of arithmetic operations (broken down by adds, subtracts, multiplies, and divisions) associated with only the Post Detection Process are counted.

After the specified number of monte carlo runs are completed, the results stored by the bookeeping are averaged and outputted as measures of effectiveness (MOE's). A list of the output MOE's are

- Probability of a target being rejected through the deghosting algorithm
- Ghosting ratio (ratio of ghosting probability to the quiescent false alarm probability)
- Number of Operations (broken down by additions, subtractions, multiplication, divisions)
- Total probability of a false alarm, P_{FA}

- The minimum required signal-to-noise ratio per pulse burst, $(S/N)_{req}$, needed to achieve the desired P_F and P_D ($(S/N)_{req}$ is the average power).

- Number of Operations per second required.

Note that $(S/N)_{req}$ is not only a MOE but a computed input system parameter.

PDPMOD consists of approximately 2500 lines of Fortran 77 code designed to run on a Digital Equipment Vax 11/730 Minicomputer. The execution time of one monte carlo iteration varies greatly with the selected outputs.

V. SUMMARY

A computer model which simulates a Multiple High PRF Pulse Doppler radar has been developed. The model has the capability of computing the system parameters and Post Detection Processing necessary to achieve a given desired probability of detection and false ala

A variety of parameters such as range resolution, number of PRF bursts, number of doppler bins, and Swerling model are inputted. Output measures of effectiveness include the required signal-to-noise power ratio per pulse burst, average number of a arithmetic operations, and ghosting probabilities.

VI. REFERENCES

1. W.A. Skillman and D.H. Mooney, "Multiple PRF Ranging," Proc. IRE Fifth Natl. Conf. Military Electronics, 1960, pp. 37-40. Reprinted in *CW and Doppler Radar,* Vol. 7, Radars, ed. D.K. Barton, Dedham, MA: Artech House, pp. 205-214.

2. S.A. Hovanessian, "An Algorithm for Calculation of Range in a Multiple PRF Radar," *IEEE Trans. Aerospace and Electronic Systems,* Vol. AES-12, No. 2, March 1976, pp. 287-290.

3. Karl Gerlach, T.B. Mitchell, G.A. Andrews, "Deghosting Algorithms for a Multiple High PRF Radar," NRL Report 8808, publication pending.

4. Karl Gerlach, T.B. Mitchell, G.A. Andrews, "Cascaded Detection Processing for a Multiple High PRF Pulse Doppler Radar," NRL Report 8830, publication pending.

5. J.V. DiFranco and W.L. Rubin, Radar Detection, Artech House Inc., Dedham, MA, 1980.

6. H.L. Van Trees, Detection, Estimation, and Modulation Theory, Vol. I, John Wiley and Sons Inc., New York, 1968.

Appendix A

MULTIPLE PRF RANGING

I. INTRODUCTION

In order to resolve a target's range ambiguity that is caused by using a high PRF, multiple PRF's are employed; i.e., the PRF is changed from one pulse burst to another. This appendix describes procedures for finding the unambiguous range from the PRF returns. Other references include [1-3].

The principles involved in a two-PRF ranging system are shown in Fig. A1. In this system, the ambiguous range to the target is determined first in PRF No. 1, and then the ambiguous range is redetermined in PRF No. 2. By taking a time comparison of the two ambiguous ranges, made possible by synchronism of the PRF's, a coincidence pulse is obtained which is a measure of the true range.

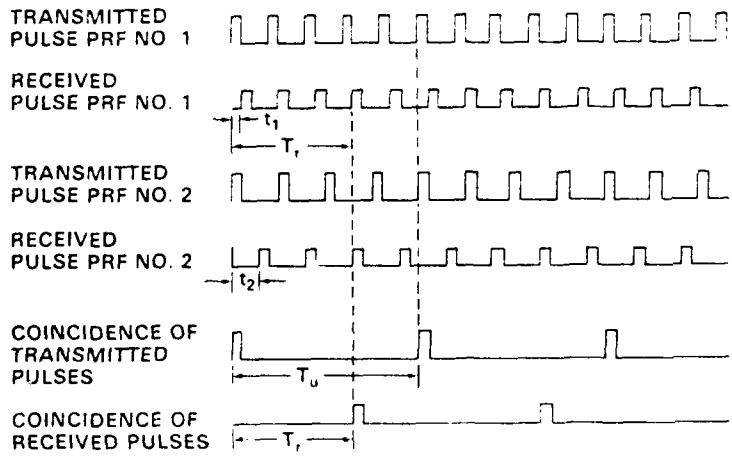

Fig. A1 — Principles of two PRF ranging

As shown in the figure, the PRF's are chosen to have a common submultiple frequency. If the transmitted pulse trains are then compared in a coincidence detector, the common submultiple frequency is obtained. Similarly, if a range track is established on the target first at one PRF and then the other, comparison of the range gates gives the same submultiple frequency, but shifted in time. By measuring the time delay between the two sets of coincidence pulses, the true target range is obtained.

II. MATHEMATICAL MODELING OF PRF RANGING

A mathematical approach to finding the unambiguous range, R, of a target can be formulated as follows. Let the ambiguous ranges of the target associated with the first and second PRF bursts be r_1 and r_2, respectively. Also let Δr be the range resolution of the radar system, and PRI_1, PRI_2 be the pulse repetition time interval (PRI) of the two PRF's. Thus

$$PRI_i = \frac{1}{PRF_i} \; ; \; i = 1, 2. \tag{A1}$$

Note that the time delay resolution capability, Δt, of the radar system is related to the range resolution by the formula

$$\Delta t = \frac{2\Delta r}{c} \tag{A2}$$

where c is the speed of light.

If we quantize the ranges into range resolution cells by indexing them to integers, then we can define the indices m_1, m_2 and M associated with ranges r_1, r_2, and R respectively as

$$m_i = \left[\frac{r_i}{\Delta r}\right]; \quad i = 1,2 \tag{A3}$$

and

$$M = \left[\frac{R}{\Delta r}\right] \tag{A4}$$

where $[\cdot]$ is the least integer function; i.e., $[3.4] = 3$.

The total number of range cells in the first and second PRI's are

$$P_i = \left[\frac{\text{PRI}_i}{\Delta t}\right]; \quad i = 1,2 \tag{A5}$$

respectively.

The integer M which is associated with the target's unambiguous range and the integer's m_1 and m_2 which are associated with the target's ambiguous ranges are related to one another by the integer equations

$$M \equiv m_1 \bmod P_1 \tag{A6a}$$

$$M \equiv m_2 \bmod P_2 \tag{A6b}$$

where the "mod" notation signifies that there exists integers k_i, $i = 1,2$ such that

$$M = m_1 + P_1 k_1 \tag{A7a}$$

$$M = m_2 + P_2 k_2. \tag{A7b}$$

The Chinese Remainder theorem guarantees that if P_1 and P_2 are relatively prime integers, then the system of equations given by (A6) has a solution and that the solution is unique. Hence for a two PRF radar system, if we measure r_1 and r_2 and know Δr a priori, then a solution for R can be formulated using (A3), (A5), (A6), and the equation

$$R = M\Delta r. \tag{A8}$$

It can be shown that the solution of (A6) is given by the equations

$$M = (a_1 m_1 + a_2 m_2) \bmod P_1 P_2 \tag{A9}$$

and

$$a_1 = P_2 x_1 \equiv 1 \bmod P_1 \tag{A10a}$$

$$a_2 = P_1 x_2 \equiv 1 \bmod P_2 \tag{A10b}$$

where x_i, $i = 1,2$ are the lowest integers satisfying each equation.

This ranging technique can be extended to using more than two PRF's. If N PRF's are used and $r_1, r_2, \ldots, r_N$ are the ambiguous ranges of target at range R then

$$M \equiv m_i \bmod P_i;\ i = 1, 2, \ldots N \tag{A11}$$

where m_i, $i = 1, \ldots, N$ are the range indices associated with the ambiguous ranges, $P_i = [\mathrm{PRI}_i/\Delta t]$, $i = 1, \ldots, N$, and $P_1 < P_2 < \ldots < P_N$.

However, for the multiple PRF radar system described in the main text, the extra PRF's above two are redundant for determining a target unambiguous range; i.e. the range extent of the radar's mainbeam footprint is such that only two PRF bursts are necessary to determine the unambiguous range of a given target ($M \leqslant P_1P_2$). One of the purposes of the extra PRF's is to determine the unambiguous range of a target if two or more targets fall within the same doppler bin.

For example, for a 3 PRF system, let there be two targets in the same doppler bin and let the targets be at unambiguous ranges, R_1 and R_2 respectively. If the ambiguous range cell indices (ARCI's) associated with R_1 and R_2 are $m_1^{(1)}$, $m_2^{(1)}$, $m_3^{(1)}$ and $m_1^{(2)}$, $m_2^{(2)}$, and $m_3^{(2)}$ respectively then

$$\begin{aligned} M_1 &\equiv m_i^{(1)} \bmod P_i \quad i = 1,2,3 \\ M_2 &= m_i^{(2)} \bmod P_i. \end{aligned} \tag{A12}$$

However, in the post detection processor, we are given only the knowledge that there are detection reports in the $m_1^{(1)}$, $m_2^{(1)}$, $m_3^{(1)}$, $m_1^{(2)}$, $m_2^{(2)}$, and $m_3^{(2)}$ range bins. In order to associate $m_1^{(1)}$, $m_2^{(1)}$, and $m_3^{(1)}$ with target 1, we use the range redundancy to find a single range, R_1, associated with these ambiguous ranges. Any other triplet of unambiguous ranges would not yield a unique solution to (A12) such that $M_1 \leqslant P_1P_2$.

Appendix B

RANGE AND TARGET AMBIGUITY RESOLUTION ALGORITHM

I. INTRODUCTION

This appendix describes the range and target ambiguity (RTAR) algorithm that has been developed for the PDP of Pulse Doppler Radar presented in the text. The RTAR algorithm is necessitated by the use of multiple PRF bursts which resolve range ambiguities. Appendix A describes the multiple PRF ranging technique and is background reading material for this appendix.

The basic PDP configuration is illustrated in Figs. 1-5. A "one" entry in D-MEM at memory position i,j indicates a detection at ambiguous range r_{mn} where m is the index of the range resolution cell and n is the PRF burst index.

The RTAR algorithm searchs D-MEM for detections and constructs a pseudo matrix of ambiguous range cell indices (ARCI). For example if $m_{n1}, m_{n2}, \ldots, m_{nk_n}$ are the ARCI's for nth pulse burst, where k_n is the number of detections in D-MEM for the nth PRF burst, then this pseudo matrix appears as seen below

$$\begin{array}{c|ccccc} \mathrm{PRF}_1 & m_{11} & m_{12} & m_{13} & \cdots & m_{1k_1} \\ \mathrm{PRF}_2 & m_{21} & m_{22} & m_{23} & \cdots & m_{2k_2} \\ \vdots & \vdots & \vdots & \vdots & \vdots & \vdots \\ \mathrm{PRF}_N & m_{N1} & m_{N2} & m_{N3} & \cdots & m_{Nk_N}. \end{array}$$

Note that the matrix need not be rectangular since the k_i need not be equal (hence, the terminology pseudo matrix).

The detections as indicated by this pseudo matrix may be from real targets or from false alarms which result because of internally or externally generated noise. If a target is located at unambiguous range, R, which is uniquely associated with the unambiguous range resolution cell, M, and the ARCI's associated with this range are $L_1, L_2, \cdots L_N$, i.e.,

$$M \equiv L_n \bmod P_n;\ n = 1, 2, \ldots N$$

(see Appendix A), then some or all of these values will be embedded in the pseudo matrix. All of them may not be there because the target may not have the necessary received signal power on receive for a given PRF burst to be detected at the first threshold level as seen in Fig. 5.1.

If at least M of the N PRF burst returns for a given target are detected by the first level threshold then it is the task of the RTAR algorithm to sift through the detections (real and false) in the pseudo matrix, find the subset of $\{L_1, L_2, \ldots, L_N\}$ embedded in this matrix, and associate them with a target while at the same time discover the target's unambiguous range. The uniqueness of a given target as embedded in this matrix is highly probable due to the fact that the extra PRF bursts above two are redundant (see Appendix A). By this we mean that the maximum operating range of the radar is such

that any two of the PRF bursts can determine the unambiguous range of a given target assuming that the returns from the two PRF's are above the first level threshold. The extra PRF's are used to resolve target ambiguities that can occur when more than one target is in a given doppler bin. Note that if this redundancy did not exist that the target ambiguities could not be resolved and false alarms (ghosts) would be generated.

II. ALGORITHM DESCRIPTION

The algorithm works as follows. After the pseudo matrix has been constructed from the information contained in D-MEM, element m_{11} is chosen as the seed element. All unambiguous ranges associated with m_{11} and each element of the succeeding PRF rows are generated; i.e.,

$$\left.\begin{array}{ll} (m_{11},m_{21}) & \rightarrow R_{21} \\ (m_{11},m_{22}) & \rightarrow R_{22} \\ \vdots & \\ (m_{11},m_{2k_2}) & \rightarrow R_{2k_2} \end{array}\right\} \text{PRF 2 row}$$

$$\left.\begin{array}{ll} (m_{11},m_{31}) & \rightarrow R_{31} \\ (m_{11},m_{32}) & \rightarrow R_{32} \\ \vdots & \\ (m_{11},m_{3k_3}) & \rightarrow R_{3k_3} \end{array}\right\} \text{PRF 3 row}$$

$$\vdots$$

$$\left.\begin{array}{ll} (m_{11},m_{N1}) & \rightarrow R_{N1} \\ (m_{11},m_{N2}) & \rightarrow R_{N2} \\ \vdots & \\ (m_{11},m_{Nk_N}) & \rightarrow R_{Nk_N} \end{array}\right\} \text{PRF } N \text{ row}$$

Next the sets

$$S_n = \{R_{n1},R_{n2}, \ldots, R_{nk_n}\};\ n = 2, \ldots, N$$

are formed. Following the formation of these sets, a search routine looks for and records the number of times a range occurs among all of the sets. The unambiguous ranges that occur are ordered by their frequency. If an unambiguous range occurs at least M times, then a candidate target is declared at that unambiguous range.

When this sequence of the algorithm is complete the m_{11} element is eliminated from the pseudo matrix and thus the pseudo matrix is reduced in the number of elements by one. Hence, the above procedure can be reiterated until the number of elements in the pseudo matrix is zero.

The choice of the succeeding seed is based on the following procedure. If an element exists to the right of the current seed, then this element is chosen as the next seed (for example, seed = m_{12}); if this element does not exist, then the seed is chosen from the far left element of the succeeding PRF row (for example, seed = m_{21}). If the succeeding PRF row contains no elements, then the next PRF row that does contain at least one element is found, and its far left element is chosen as the next seed.

The algorithm is terminated when the number of PRF rows that have at least one element is less than M because there is no possibility of a candidate target being declared.

Also the algorithm checks to make sure multiple candidate targets for the same target are not generated. This can occur as follows. If $(L_1, L_2, \ldots, L_N)$ is a valid set of ARCI's for a given target, then $(L_2, L_3, \ldots, L_N)$ is also a valid set. Hence, if $(L_1, L_2, \ldots, L_N)$ were embedded in the original psuedo matrix, then the ARCI's $(L_1, L_2, \ldots, L_N)$ can be associated with a candidate target as can $(L_2, L_3, \ldots, L_N)$. However, the algorithm checks for this condition and only single candidate targets are generated.

Note that we have chosen to call the valid detections resulting from the binary detection process (M out of N detector) "candidate targets." This is due to the fact that the candidate target's returns (in VMEM) must still be tested by the incoherent integrator detector. In addition, the detections generated by the incoherent integrator are inputted into a deghosting algorithm which attempts to eliminate any of the ghosts which could have been generated by the RTAR algorithm. The deghosting algorithm is discussed further in Appendix D.

Appendix C

PDP DETECTION THRESHOLDS

I. INTRODUCTION

The equations necessary to solve for the three detection thresholds seen in Fig. 1 are formulated in this appendix. Embedded in the post detection processor (PDP) is a binary detector followed by an incoherent integrator detector (often referred to as a square law detector).

We simplify the analysis by considering the hypothesis that a target at a given unambiguous range, R, is detectable. Let the ambiguous ranges associated with R be $r_1, r_2, \ldots r_N$ where N is the number of PRF bursts used. Let the voltage returns from the range-doppler cells seen in Fig. 2 for each ambiguous range be $v_1, v_2, \ldots, v_N$ respectively. Note that v_n, $n = 1, \ldots, N$ can be extracted from V-MEM.

The hypothesis that a target exists at range R can now be tested using the simplified detector as seen in Fig. C1. In this figure, we see that a M out of N binary detector is cascaded with a square law detector. Recall that the binary detector is used to resolve range and target ambiguities. If the candidate target passes the binary detector test, then the voltage returns are squared in magnitude and incoherently added and tested against a third threshold. The square law detector enhances detection since a smaller *average* signal-to-noise power ratio (S/N) per pulse burst is required for a square law detector than a binary detector for a given probability of detection and false alarm. (Note that S/N is defined as average signal-to-noise power ratio and not the peak average.)

If we select an output probability of false alarm and a probability of detection, (measured at the output of the square law detector) then it is possible to choose the thesholds, T_1, T_2, and T_3 and a minimum (S/N) such that these system performance measures are achieved.

II. BINARY DETECTOR THRESHOLDS

The minimum required (S/N) per pulse burst will also be a function of the probability at false alarm, P_{FBD}, through the binary detector as seen in Fig. C1. It can be shown [5] that the probability of detection at the output of the binary detector, P_{DBD}, and P_{FBD} are related to the probability of detection, p_d, and the probability of false alarm, p_f, at the output of the first level detector by the equations

$$P_{FBD} = \sum_{n=M}^{N} \binom{N}{n} p_f^n (1 - p_f)^{N-n} \tag{C1}$$

$$P_{DBD} = \sum_{n=M}^{N} \binom{N}{n} p_d^n (1 - p_d)^{N-n}. \tag{C2}$$

We note that P_{FBD} and p_f, are defined as "noise only" generated false alarm probability. They do not include the effects of target ghosting.

Now p_d will be a function of the input S/N, p_f, and the Swerling target radar cross section model assumed. For a Swerling Case II target model (pulse-to-pulse Rayleigh fluctuating incoherent pulse train), [5]

$$p_d = (p_f)^{1/(1+(S/N))}. \tag{C3}$$

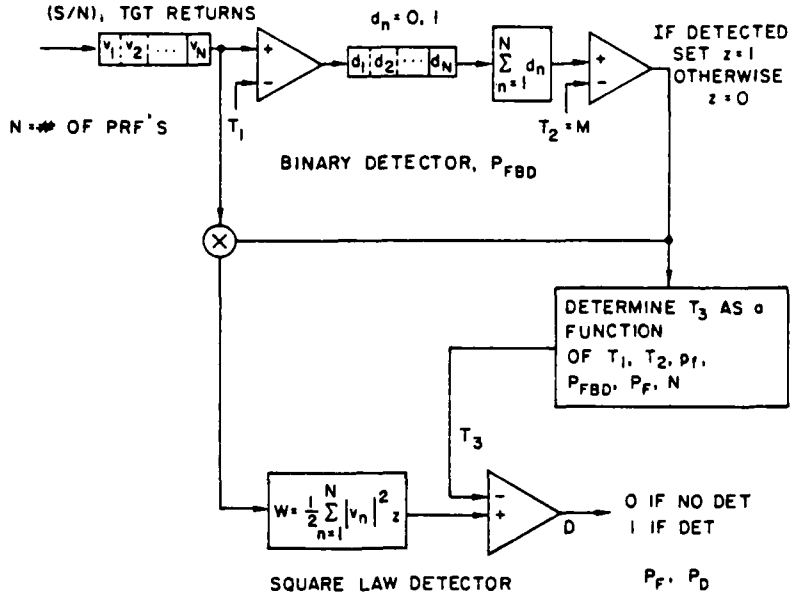

Fig. C1 — Single threshold cascaded detector

For a Swerling Case IV target model (one dominant scatterer plus pulse-to-pulse Rayleigh fluctuating incoherent pulse train),

$$p_d = \frac{1}{1 + 2/(\mathrm{S/N})}\left[1 + \frac{2}{(\mathrm{S/N})} - \frac{\ln p_f}{1 + \frac{1}{2}(\mathrm{S/N})}\right]\exp\left[\frac{\ln p_f}{1 + \frac{1}{2}(\mathrm{S/N})}\right] \tag{C4}$$

Hence if we specify P_{FBD}, S/N, and the Swerling model, we can find the M and p_f which satisfy Eq. (C1) and maximize P_{DBD}. Thus, the second threshold (which equals M), T_2, can be found.

In order to find the first threshold, T_1, it can be shown [4] that

$$p_f = e^{-\frac{T_1^2}{2}}. \tag{C5}$$

Therefore, if p_f is known, T_1 can be solved for using (C5).

Note that we are assuming that the thresholds T_1 and T_2 which minimize the required S/N for the cascaded PDP are the same as the T_1 and T_2 that minimize the required S/N for the binary detector. Intuitively this is true because the binary detector is cascaded with the square law detector so that any loss of detection in the binary detector caused by using other thresholds will be passed along to the square law detector.

Also note that it may be necessary to set a lower bound, L_{MIN}, on T_2 such that $T_2 \geq L_{\mathrm{MIN}}$ in order to have a minimum number of returns to resolve range and target ambiguities. For example, if $N = 4$, $P_{FBD} = 10^{-6}$, (S/N) = 10 dB, and a Swerling Case IV target model, then it will be found that $T_2 = 2$ for maximum detection. However if it is necessary to have at least three returns to resolve range and target ambiguities, then T_2 is set equal to three and a p_f is calculated which satisfies (C1). Using (5), T_1 is found. For this case, it can be shown that there is approximately a 5% loss in the probability of detection at the output of the square law detector P_D, if $T_2 = 3$ instead of $T_2 = 2$.

III. SQUARE LAW DETECTOR THRESHOLD

The value of the third threshold, T_3, as seen in Fig. C1 will be a function of p_f, P_{FBD}, N, T_1, and M (T_2). Note that T_3 is not a function of the P_D because we are using the Neyman-Pearson criteria [6] whereby T_3 is chosen such that the probability of false alarm, P_F, is kept constant.

From the functional block diagram of the cascaded detector seen in Fig. C1 we see that T_3 can also be chosen as a function of the number of times, L, that a candidate target was detected by the binary detector. Hence, a different T_3 can be calculated for each value of $L \geq M$. The technique of using a calculated value of T_3 for each L is called a Multiple Threshold Cascaded Detector (MTCD). A block diagram of this configuration is seen in Fig. C2.

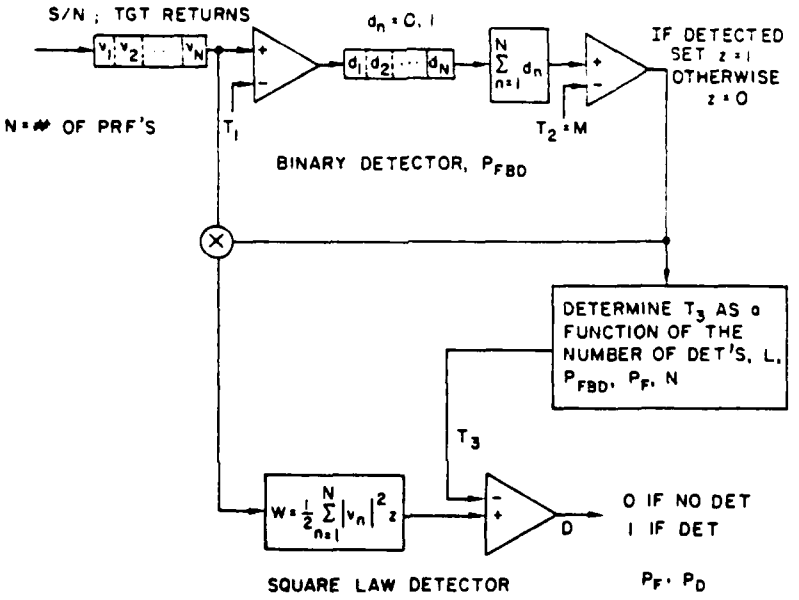

Fig. C2 — Multiple threshold cascaded detector

It is also possible to calculate a single threshold, T_3 for all $L \geq M$, and still attain the desired P_F. This configuration is seen in Fig. C1 and will be called a Single Threshold Cascaded Detector (STCD). It was found that there was very little difference in performance between the STCD and MTCD for a given P_F, P_{FBD}, and P_D. Therefore a STCD was selected due to its simplicity.

It is shown in Ref. [4] that the third threshold, T_3, for an STCD can be found by solving the following equation for T_3:

$$P_F = c \sum_{L=M}^{N} \sum_{k=0}^{N-L} (-1)^k \binom{N-L}{k} G_{kL}(T_3) P_{FBD}(L) \tag{C6}$$

where the function $G_{kL}(T_3)$, $k = 1, 2, \ldots, N - L$ is defined as

$$G_{kL}(T_3) = \begin{cases} e^{-k.5T_1^2} & \text{if} \quad T_3 \leq (k+L).5T_1^2 \\ e^{-(T_3 - L.5T_1^2)} \sum_{h=0}^{N-1} \dfrac{(T_3 - (k+L).5T_1^2)^h}{h!} & \text{otherwise} \end{cases} \tag{C7}$$

Also

$$c = \frac{1}{(1 - e^{.5T_1^2})^{N-L}}. \tag{C8a}$$

and

$$P_{FBD}(L) = \binom{N}{L} p_f^L (1 - p_f)^{N-L} \tag{C8b}$$

Obviously, a computer search for T_3 is necessary in order to find a solution.

IV. DISCUSSION

In order to specify a required (S/N) per pulse burst for a given P_D and P_F, it was necessary to run a computer simulation of the STCD processor. In this monte carlo simulation, P_{FBD}, S/N per pulse burst, N, and P_F were inputted, then T_1, T_2, and T_3 were calculated using the previously described procedure. The voltage returns, v_n, $n = 1, 2, \ldots, N$ were randomly generated given the (S/N) per pulse burst and Swerling target models; and then inputted into an STCD processor with system parameters T_1, T_2, and T_3. Detections were recorded at the output of the square law detector and averaged over a number of monte carlos in order to estimate the output probability, P_D. The values of P_D were calculated as a function of a stepped (S/N) so that a selected P_D could be matched with the required (S/N) necessary to achieve that P_D.

For example, contours of estimated P_D versus (S/N) and P_{FBD} can be seen in Fig. C3 with other parameters listed in this figure. For a desired $P_D = .9$, $P_F = 10^{-10}$, and $P_{FBD} = 10^{-4}$, we see that the required (S/N) is approximately 11.3 dB. The relative accuracy of the probability of detection, σ, can be found using the formula

$$\sigma = \sqrt{\frac{P_D^{-1} - 1}{N_{mc}}} \tag{C9}$$

where N_{mc} is the number of monte carlos. For 10000 monte carlos and $P_D = .9$, $\sigma = .003$. Note that $M = 3$ for the M out of N binary detector. We constrained M to be greater than or equal to three and then computed the optimal binary detector thresholds.

If we specify a desired $P_D = .9$ and $P_F = 10^{-10}$, then it is possible using Fig. C3 to find the minimum required signal-to-noise power ratio, (S/N), which will achieve these performance measures for each value of P_{FBD}.

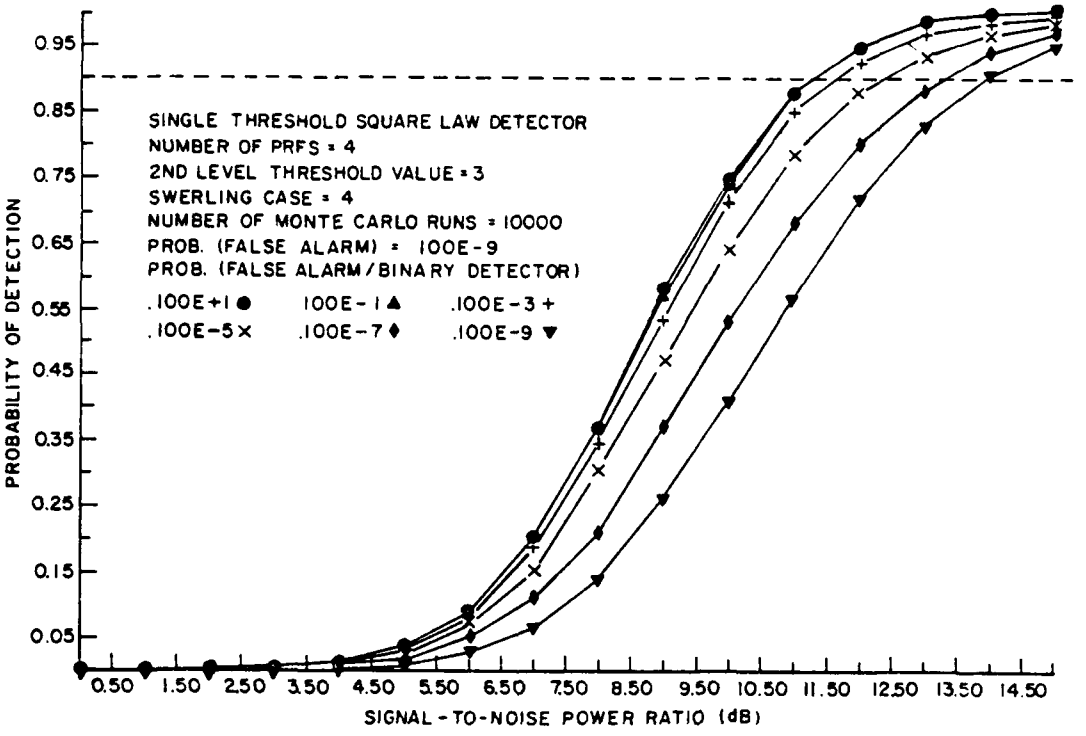

Fig. C3 — Probability of detection vs signal-to-noise

Appendix D

DEGHOSTING ALGORITHM

I. INTRODUCTION

This appendix reviews in detail an algorithm that was developed to eliminate many of the ghosts that could be generated by the Range and Target Ambiguity Resolver algorithm (RTAR). A ghost is a false target that is generated by associating noise only returns with real target returns. More specifically, ghosts are created as a result of

1. taking at least one real target return that is contained in V-MEM (see Fig. 2) which is detectable through the first level threshold of the binary detector,

2. possibly combining this with returns in V-MEM which contain noise only and which are detectable by the first level threshold,

3. so that the number of combined false returns and real target returns is greater than or equal to M,

4. such that the ambiguous range cell indices (ARCI's) associated with these returns can be associated with a unique unambiguous range,

5. and the sum of the squares of these returns passes the square law detector threshold, T_3.

An example of ghosting is illustrated in Table D1. In this table, we have tabulated the output of the RTAR algorithm for a simulated input data set under noisy conditions. In this example there were four targets contained within a given doppler bin. After processing through the RTAR algorithm (with the embedded binary detector) and the square law detector, we see from this table that eight candidate targets (CTGT) were generated. The first four listed in this table are real targets and the last four are ghosts. The number of PRF's used was 5, and the PRI indices associated with these PRI's are $P_1 = 34$, $P_2 = 35$, $P_3 = 37$, $P_4 = 39$, and $P_5 = 41$ (see appendix A for multiple PRF ranging techniques). In this table, we have tabulated the ARCI's for each candidate target versus the PRI indices. The number "−1" seen in this table indicates no detection for a given CTGT for that particular PRI. Note that the binary detector used was a 3 out of 5 detector ($M = 3$).

Table D1 — Ambiguous Ranges vs. PRI Indices and Candidate Target Number

	PRI Indices					
	P_1	P_2	P_3	P_4	P_5	
CTGT	34	35	37	39	41	# DET's
1	3	34	−1	22	16	4
2	11	8	−1	35	31	4
3	22	17	7	36	28	5
4	31	−1	−1	26	24	3
5	3	−1	7	26	−1	3
6	11	17	−1	22	−1	3
7	31	−1	7	−1	16	3
8	−1	34	−1	35	24	3

Also note that all of the ghosts, CTGT's 5, 6, 7, 8, have taken returns from the real targets, and that no ghost contains a "noise only" return. For example, the ghost, CTGT 5, stole one return from CTGT 1 (ARCI = 3 for $P_1 = 34$), one return from CTGT 3 (ARCI = 7 for $P_3 = 37$), and one return from CTGT 4 (ARCI = 26, $P_3 = 39$). It can be shown that the unambiguous range associated with the ARCI's of this ghost is 377; i.e.,

$$\begin{aligned} 377 &\equiv 3 \bmod 34 \\ 377 &\equiv 7 \bmod 37 \\ 377 &\equiv 26 \bmod 39 \end{aligned} \tag{D1}$$

II. DEGHOSTING ALGORITHM CONSIDERATIONS

The purpose of the deghosting algorithm (see in Fig. 1) is to eliminate many of the ghosts that are generated by the RTAR algorithm while at the same time eliminating only a small percentage of real targets. The latter statement is the constraint which does not allow us to have perfect deghosting. Hence there are two measures of effectiveness of a deghosting algorithm. These are

- P(Ghost/Target) = probability that a real target will be called a ghost and hence not detected
- P(Ghost) = Probability that a ghost will not be deghosted and hence be detected as a target

For the deghosting algorithm to be presented, the measures of effectiveness are discussed in the following and the "goodness" of the algorithm is verified.

(U) The basis of the methodology of the deghosting algorithm lies in making the following two observations:

1. ghosts tend to consist of stolen ambiguous range detections from real targets rather than false alarms in V-MEM (see Fig. 2)

2. ghosts tend to have fewer detections associated with them than real targets

The second observation results because the probability of a ghost with more than M detections is much smaller than a probability of a ghost with exactly the minimum number of detections, M. For example, listed in Table D1 are the number of detections for each candidate target. Note that the ghosts (CTGT's 5, 6, 7, 8) have exactly the minimum number of detections, 3, and that the number of detections for real targets (CTGT's 1,2,3,4) ranges from 3 to 5.

Hence, a deghosting algorithm should treat candidate targets with more detections in such a way that these CTGT's are harder to eliminate than those with less detections.

For the deghosting algorithm that was developed, we measure the number of "range matches" that a candidate target has with a set, C, of other candidate targets. A "range match" occurs when a selected ARCI at each PRI index of the CTGT is identical with any other ARCI's of set C at that PRI index. For example, using Table D1, if the selected CTGT is CTGT 5 and

$$C = \{\text{CTGT's } 1, 2, 3, 4, 6, 7, 8\} \tag{D2}$$

then CTGT 5 has 3 range matches. For $P_1 = 34$, CTGT 5's ARCI = 3 and matches with CTGT 1's ARCI = 3. For $P_3 = 37$, CTGT 5's ARCI = 7 and matches with CTGT 3 ARCI = 7 and CTGT 7's

ARCI = 7. For $P_4 = 39$, CTGT 5's ARCI = 26 matches with CTGT 4's ARCI = 26. Note that for $P_3 = 37$, that there are two range matches but that by our definition this counts as only one range match.

In the deghosting algorithm that follow, we will eliminate CTGT's based on their number range matches with another set of candidate targets. If the number of range matches is R_M, then the candidate target will be called a ghost if

$$R_M \geq G \triangleq D - M + 2 \tag{D3}$$

where D equals the number of detections of the candidate target and G is a lower bound defined by (D3). Note from this inequality that candidate targets with more detections are less likely to be eliminated (or deghosted) because G increases as D increases. As mentioned previously, it was found through simulation that a large percentage of the ghosts have M binary detections associated with them. A much smaller percentage of ghosts have $M + 1$ binary detections and an even much smaller percentage have $M + 2$ binary detection.

For example, for the 3 out of 4 binary detector the most common ways that a ghost can pass through the deghoster algorithm that is subsequently described are:

1. A ghost steals 4 ambiguous ranges from the candidate targets that are real targets

2. A ghost steals 1 ambiguous range from the candidate targets that are real targets and 2 ambiguous ranges from real targets that are not detected

3. A ghost steals 1 ambiguous range from the candidate targets that are real targets, 1 ambiguous range from a real target that is not detected, and uses a false detection in an ambiguous range from V-MEM.

4. A ghost uses 2 false detections in ambiguous ranges from V-MEM and steals 1 ambiguous range from the candidate targets that are real targets.

For a 3 out of 4 binary detector, the undetected real targets cause most of the ghosts. Hence, increasing the required S/N will decrease the ghosting probability.

In fact it can be shown that if all the real targets are detected through the square law detector then using a lower bound, G, as defined by (D3) implies that if a ghost is not deghosted (and hence detected as a target which results in a false alarm), then the number of false alarm (or noise only) returns that are detected by the first level threshold and associated with a candidate target is greater than or equal to $M - 1$. Hence, the probability of a ghost being declared a target, P (Ghost), is dependent on at least $M - 1$ false alarms in V-MEM which can be associated with one unambiguous range. The probability of this occurring is slightly greater than the probability of M "noise only" returns which can be associated with one ambiguous range being declared a target.

In order to see that a ghost which is not deghosted must contain at least $M - 1$ false detections, under the assumption that all targets are detected, consider a candidate target which is a ghost which has D detections and $D - M + 1$ range matches (one more and the ghost would be declared a ghost) as seen in Fig. D1. From this figure it is evident that there must be exactly $M - 1$ detections which are due to "noise only" returns.

If G were set equal to $D - M + 1$, then it could be shown that at least M false detections (noise only) are necessary to produce a ghost, assuming all real targets were candidate targets. It would seem desirable to set G equal to $D - M + 1$ because then intuitively the probability of ghosting would be approximately equal to the quiescent probability of flase alarm (noise only generated false targets).

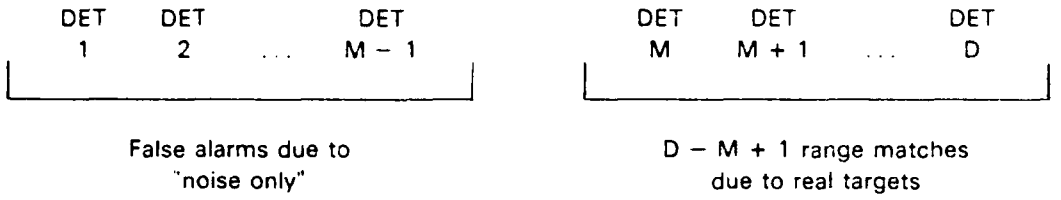

Fig. D1 — A ghost with D detections and $D - M + 1$ ranges matches

However it can be shown [3] that for $G = D - M + 1$ the probability that a target is classified a ghost by the deghosting algorithm becomes significant. Thus, target detection capability is severely degraded. For $G = D - M + 2$, it can be shown [3] that target detection capability is only slightly affected.

For a given M out of N binary detector a list of the most common ways that a ghost can occur can be constructed as it was done for the 3 out of 4 cases. For each ghosting event, a probability of ghosting can be formulated. Reference [3] contains closed formed solutions of ghosting and deghosting probabilities for the 3 out of 4 case.

III. DEGHOSTING ALGORITHM DESCRIPTION

A functional flow diagram of the deghosting algorithm is shown in Fig. D2. This deghosting algorithm is easily implemented and described. Each of the candidate targets are sequentially range matched against each of the other candidate targets. If the number of range matches, R_M, is greater than $G = D - M + 2$, where D is the number of binary detections of the selected CTGT, then the CTGT is declared a ghost. Otherwise, it is declared a target.

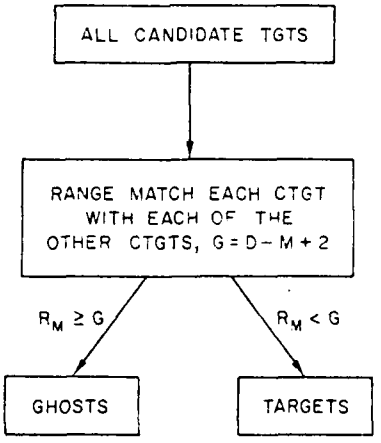

Fig. D2 — Flow diagram of deghosting algorithm

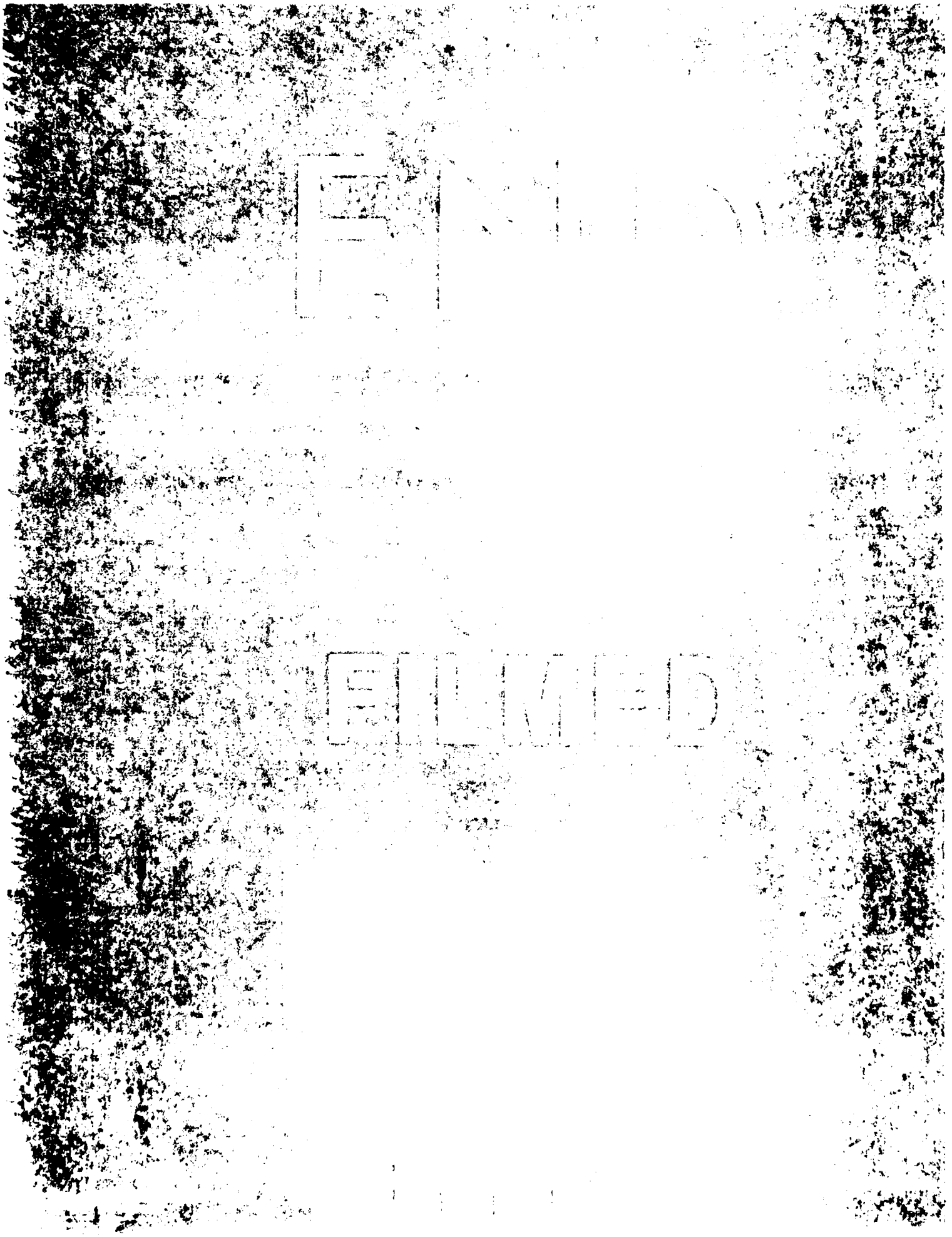
UNCLASSIFIED